EVALUATION OF ULTRASONIC C-SCAN ATTENUATION IMAGE

T. Wang† and J. Saniie*

†Physical Acoustic Corporation
15 Princess Road, Lawrenceville, NJ 08648

*Electrical and Computer Engineering Department
Illinois Institute of Technology, Chicago, IL 60616

ABSTRACT

In the ultrasonic NDE of materials, peak echo value in a time window corresponding to a given depth of the material is often used to generate C-Scan images. Peak echo C-Scan images represent integrated properties of the transducer impulse response, sound propagation path, and the scattering and absorption characteristics of materials. Therefore, it is inaccurate to assume that the resulting image presents the properties of a local area. In this study, temporal averaging and homomorphic processing, which extract the local ultrasonic wavelet and estimate the attenuation coefficient, have been incorporated into C-Scan imaging to generate an attenuation map. The variation of this map displays changes in the scattering cross section and in the absorption of materials. These processing schemes are implemented into an integrated software package designed to yield a high resolution C-Scan attenuation image. Experimental results have shown that for a composite sample with fatigue damage caused by compression, the C-Scan attenuation map provides an improved image of the damaged area over the conventional peak detection scheme. The benchmark of image quality (i.e., average pixel value of the damaged area over average pixel value of the non-damaged area) indicates that the C-Scan attenuation map outperforms the peak-echo C-Scan by a factor higher than two to one.

INTRODUCTION

It is well known that the magnitude and phase of ultrasonic echoes is closely related to the inherent elastic and structural properties of the examined specimen. In conventional C-Scan testing (e.g., composites) the presence of defects such as cracks, voids, impact damage, and delaminations are determined by displaying peak echo amplitude in the region of interest in the form of a multilevel or color-coded two dimensional image. Recently, there have been efforts to improve the resolution of the image by incorporating phase information, using deconvolution, or by focusing beam at a desired depth. In most cases, these approaches work well, although, they represent information related to the entire sound propagation path which may mask the desired information pertaining to a selected region of the material. Any potential inhomogeneity on the sound path can greatly alter the final results causing false alarm or misinterpretation. In this study, we present pseudo real-time attenuation map using temporal averaging, and off-line homomorphic processing to obtain local frequency dependent attenuation information for generating a color-coded attenuation map. This approach has been shown to provide a superior image of defect when compared with conventional C-Scan using peak detection.

EXPECTED ATTENUATION MAP

In this section the concept of the ultrasonic C-Scan attenuation image is presented. Energy losses result when an ultrasonic wave passes through a material. Energy losses are caused by scattering and absorption [1]. Scattering results when materials are not absolutely homogeneous. Inhomogeneities can be regarded as anything that presents a boundary within materials of different acoustical impedances such as inclusions, pores or grains. Materials exhibiting these inhomogeneities not only decrease the returned ultrasonic signal due to scattering, but also generate multiple echoes or reverberation that will lower the signal-to-noise ratio. Another cause for attenuation is absorption which results when a portion of the sound energy is converted into heat. In addition to the sound energy losses discussed above, there are other factors to consider such as losses in the coupling medium, scattering due to surface roughness and beam spreading. Therefore, attenuation is usually considered as the sum of all these factors since they all affect the amount of sound transmitted to and returned from an area of interest in the test sample. However, in many practical situations, scattering loss at ultrasonic frequencies is so much greater than the sum of other losses that the others are often considered negligible. Furthermore, the estimated attenuation coefficient [2 and 3] only presents the rate of local losses due to defect and is independent of losses resulting from the propagation path, surface roughness, and coupling medium.

The measured, backscattered echoes associated with microstructure scattering form a composite signal corresponding to many inhomogeneous reflectors with

1051-0117/91/0000-0791 $1.00 © 1991 IEEE

random amplitudes and arrival times. For example, the broadband signal corresponding to the scattering properties of a given region (e.g., region j) can be modeled as:

$$r_j(t) = \sum_{k=1}^{M} A_{kj} e^{-2\langle \alpha_j \rangle \tau_{kj}} \langle u_j(t-\tau_{kj}) \rangle \qquad (1)$$

where the term $\langle \alpha_j \rangle$ is an index representing the expected attenuation coefficient, A_{kj} and τ_{kj} represent the random amplitude and position of scatterers within the detection range associated with region j. The term $u_j(t)$ is the basic ultrasonic wavelet, and is assumed to be a Gaussian envelope,

$$\langle u_j(t) \rangle \propto e^{-\gamma_j t^2} \cos(\omega_j t) \qquad (2)$$

where ω_j is the center frequency, and γ_j is a constant representing the width of the wavelet in time.

Estimating the local expected attenuation coefficient is an important parameter for imaging local defects. In our earlier study, we performed statistical analysis for estimating this attenuation coefficient by temporally averaging the backscatterd microstructure signal. This analysis [3] can be simplified to:

$$\overline{r_j}(t) = Ce^{-\langle \alpha_j \rangle t} \qquad (3)$$

where t is time in the region of interest, and C is a lumped parameter representing the unknown local scattering cross section, the unknown propagation effect, and the unknown effect of the coupling medium. However, from the temporally averaged signal, the unknown expected attenuation coefficient can be estimated by applying linear regression after logarithmic transformation. The overall block diagram of these operations is shown in Figure 1.

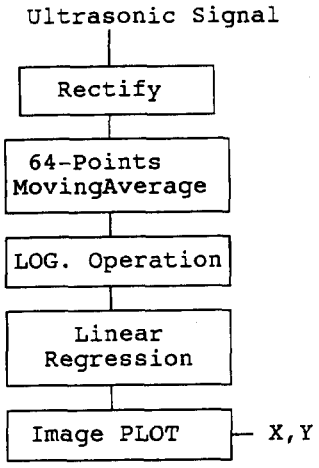

Figure 1. Block Diagram for Moving Average Attenuation Extraction Imaging System

The advantage of this method is that the estimated attenuation coefficient is independent of the propagation path, surface roughness, and the coupling medium, thus representing reliable information pertaining to the integrity of the local region of interest.

FREQUENCY-DEPENDENT ATTENUATION MAP

The measured backscattered signal as described in Equation 1 can be viewed as a superposition of many wavelets with random amplitude and arrival time representing the broadband characteristics of the ultrasonic transducer weighted by frequency dependent scattering and attenuation [2-4]. In general, by examining the wavelets, certain inherent acoustical properties of the composite signal are revealed. As shown in our previous studies [2], the ultrasonic wavelets within two adjacent regions (regions j and j+1) can be correlated to the frequency dependent attenuation coefficient,

$$\alpha_j(f) = \frac{\log|\langle U_j(f) \rangle| - \log|\langle U_{j+1}(f) \rangle|}{2\Delta d} \qquad (4)$$

where the term $\alpha_j(f)$ is the local (region j) frequency dependent attenuation coefficient due to scattering and absorption, and $\langle U_j(f) \rangle$ is the magnitude spectrum of the mean ultrasonic wavelet within the desired depth of inspection where $\Delta d = d_{j+1} - d_j$. For the clarity of the parameters and type of data involved in estimating frequency dependent attenuation see Fig. 2. As shown in our previous investigation [4], the magnitude spectrum of

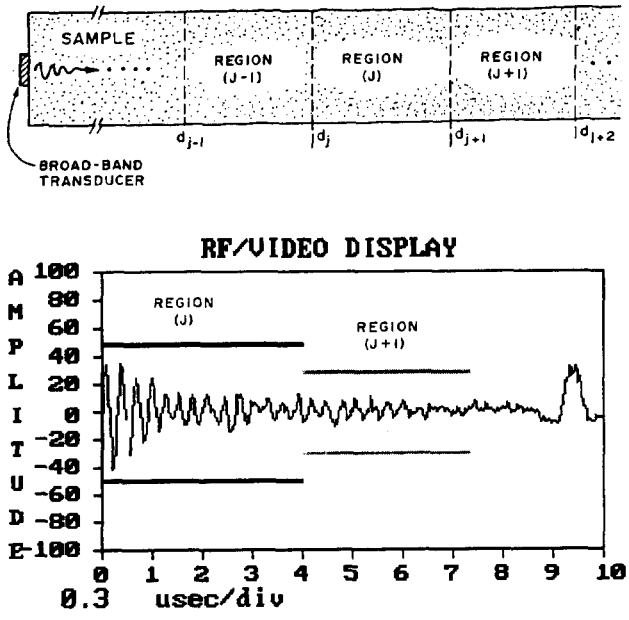

Figure 2. A Segmented Model of Ultrasonic Signal Representing Regional Characteristic of the Specimen.

the mean ultrasonic wavelets can be extracted by applying homomorphic processing to the measured backscattered signal. To characterize the frequency distribution of the attenuation coefficient, the attenuation spectrum centroid is used to construct the attenuation map. This expected frequency map represents a C-Scan image where attenuation is more dominant. The block diagram of this imaging system is shown in Fig. 3.

EXPERIMENTAL RESULTS AND DISCUSSIONS

To verify the theoretical results presented in Section II, and Section III, experiments were performed at the Physical Acoustics Corporation using an ULTRAPAC II C-Scan color imaging system. The specimen we examined was a 0.25" thick fiber reinforced carbon-carbon composite slab (4" X 7") with fatigue damage caused by compression in a cylindrical shape, 0.75" diameter and about 0.125" deep. A broadband transducer with a center frequency of 5 MHz and a 3dB bandwidth of 1.2 MHz was used for imaging the damaged area. The specimen was imaged using a gate window representing a time duration of 384 samples collected at 128 MHz. To obtain a processed image, a vast amount of RF waveforms (110 X 190 data sets to cover an area of 1.4" X 2.5") along with scanner position were acquired and stored into the system's mass storage.

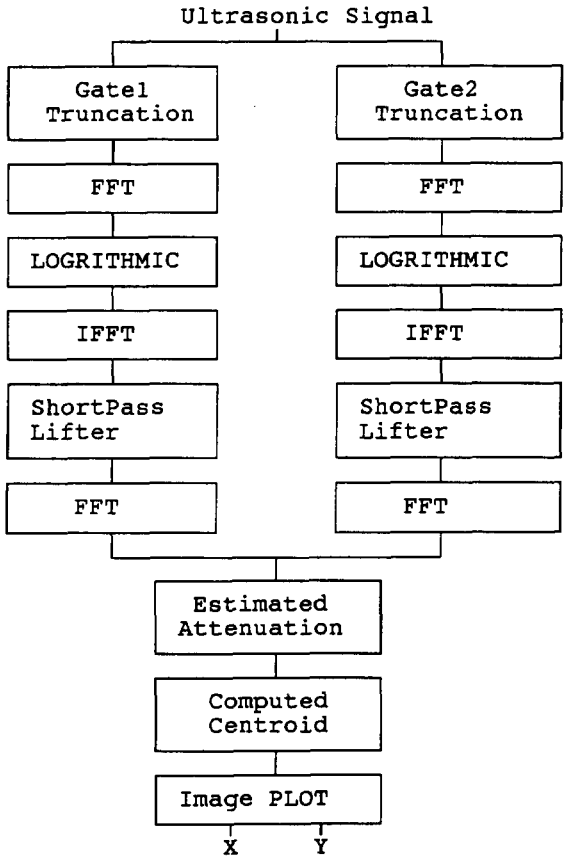

Figure 3. Block Diagram Of Homomorphic Processing for Wavelet Extraction and Attenuation Spectrum Centroid Image.

Figure 4 shows the conventional peak detection C-Scan color image obtained using the above acquired data. In addition, data were processed using a time domain moving average with a window size of 64 samples. Then, attenuation was estimated by applying the processing steps described by the block diagram presented in Figure 1. Finally, these data were used to construct the attenuation map (i.e., the image shown in Figure 5). This figure shows high sensitivity to the regional changes in the acoustical properties of the specimen. Furthermore, Figure 6 not only confirms the presence of the damaged area similar to peak detection (see Figure 5), but also displays a broader area of damage. The peak detection image has some inherent limitations when examining the regions beyond and in the vicinity of the delamination. If imaging must be conducted through a delaminated region, the returned peak value from the portion of the specimen below the delamination creates a distorted image, as is the case in Figure 4. Whereas, the expected attenuation map (Figure 5) is a representation of the material's properties regardless of the absolute intensity of detected echoes. Therefore, the attenuation map shows a higher sensitivity to the damaged region than the image based on the maximum peak value. In order to quantify and benchmark the sensitivity of these imaging methods, a contrast detection index (CDI), defined as the ratio of the average flaw intensity over the average of the background intensity, is needed. Quantitative comparison of these images indicates that the attenuation map shows a CDI with twice the value (i.e., improved sensitivity) than the conventional peak detection C-Scan image.

Figures 6 shows a C-Scan image based on attenuation spectrum centroids. This image is constructed using homomorphic wavelet extraction applied to a segmented RF signal consisting of 256 data points. As shown in this figure, the attenuation centroid map indeed displays a certain degree of improvement in sensitivity over the conventional peak detection C-Scan image. The CDI of the attenuation centroid image is almost 3 times higher than the peak detection image.

CONCLUSION

In this study we have introduced two new methods of constructing C-Scan images utilizing the attenuation coefficient in both time and frequency. These methods serve as a viable alternative or complement to the peak detection C-Scan Image. It is important to point out that estimated attenuation has a random variation, and the choice of parameters of homomorphic processing and the length of the moving average are critical to the performance

Figure 4. Peak-value C-Scan Image of a Damaged Composite Specimen.

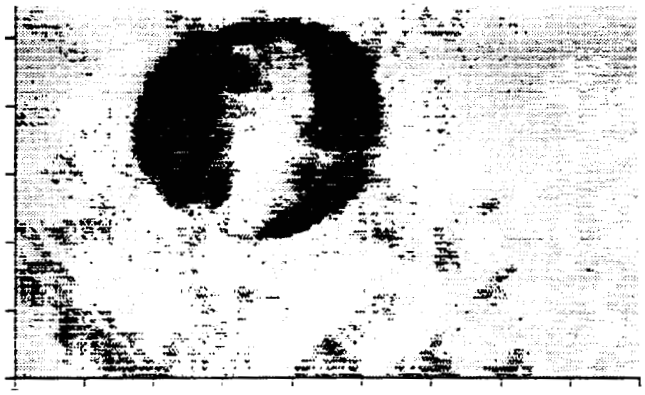

Figure 5. C-Scan Attenuation Map of a Damaged Composite Specimen Using 64-Point Moving Averaging for Attenuation Estimation.

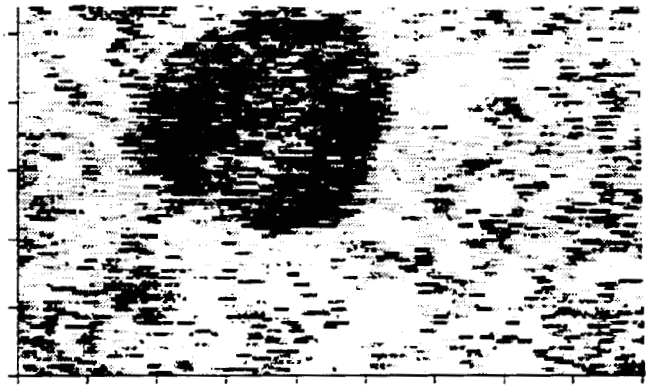

Figure 6. Homomorphic Wavelet Attenuation Centroid Image Using 256-Point Data Segments.

of the methods [2-4]. The implementation of the conventional peak detection image and the moving average attenuation map can be accomplished in real time while the scanning occurs. However, the homomorphic wavelet attenuation estimation requires a tremendous number of computations. General purpose workstations (e.g., 286 or 386 based computer with mathcoprocessor 80387) are inadequate for real-time image formation. However, with modern Digital Signal Processing (DSP) chips, the pseudo real-time implementation of homomorphic processing, estimation of frequency dependent attenuation, and the construction of an attenuation map is feasible.

REFERENCES

[1] E.P. Papadakis, "Ultrasonic Attenuation Caused by Scattering in Polycrystalline Metals", J. Acoust. Soc. Am., 37, pp.703-710, 1965.

[2] J. Saniie and N.M.Bilgutay, "Quantitative Grain Size Evaluation Using Ultrasonic Backscattered Echoes", J. Acoust. Soc. Am., 80, pp. 1816-1824, 1986.

[3] J. Saniie, T. Wang and N.M. Bilgutay, "Statistical Evaluation of Backscattered Ultrasonic Grain Signal", J. Acoust. Soc. Am., 84, pp. 400-408, 1988.

[4] J. Saniie, T. Wang and N.M. Bigutay, "Analysis of the homomorphic processing of Backscattered Ultrasonic Grain signal", IEEE Trans. on UFFC, pp. 365-375, May 1989.

[5] J. Saniie, N.M. Bilgutay and D.T. Nagle, "Evaluation of Signal Processing Schemes in Ultrasonic Gain Size Estimation", Review of Progress in Quantitative Nondestructive Evaluation, edited by D.O. Thompson and D.E. Chimenti, Vol. 5A, pp. 747-753, Plenum Press, New York, 1986.